HHS Public Access

Author manuscript

Doc Ophthalmol. Author manuscript; available in PMC 2018 June 01.

Published in final edited form as:

Doc Ophthalmol. 2017 June ; 134(3): 205–219. doi:10.1007/s10633-017-9586-x.

Pigmented and albino rats differ in their responses to moderate, acute and reversible intraocular pressure elevation

Akshay Gurdita[1], **Bingyao Tan**[2], **Karen M. Joos**[3], **Kostadinka Bizheva**[1,2], and **Vivian Choh**[1]

[1]School of Optometry and Vision Science, University of Waterloo, Waterloo, ON, N2L 3G1 Canada

[2]Department of Physics and Astronomy, University of Waterloo, Waterloo, ON, N2L 3G1 Canada

[3]Vanderbilt Eye Institute, Vanderbilt University, TN, USA, 37232

Abstract

Purpose—To compare the electrophysiological and morphological responses to acute, moderately elevated intraocular pressure (IOP) in Sprague-Dawley (SD), Long-Evans (LE) and Brown Norway (BN) rat eyes.

Methods—Eleven-week old SD (n = 5), LE (n = 5) and BN (n = 5) rats were used. Scotopic threshold responses (STRs), Maxwellian flash electroretinograms (ERGs), or ultra-high resolution optical coherence tomography (UHR-OCT) images of the rat retinas were collected from both eyes before, during and after IOP elevation of one eye. IOP was raised to ~35 mmHg for 1 hour using a vascular loop, while the other eye served as a control. STRs, ERGs and UHR-OCT images were acquired on 3 days separated by one day of no experimental manipulation.

Results—There were no significant differences between species in baseline electroretinography. However, during IOP elevation, peak positive STR amplitudes in LE (mean ± standard deviation: 259 ± 124 μV) and BN (228 ± 96 μV) rats were about 4-fold higher than those in SD rats (56 ± 46 μV) rats (p = 0.0002 for both). Similarly, during elevated IOP, ERG b-wave amplitudes were 2-fold higher in LE and BN rats compared to those of SD rats (947 ± 129μV & 892 ± 184 μV, vs 427

Corresponding author: Vivian Choh, vchoh@uwaterloo.ca.

DISCLOSURES

Funding: This work was funded in part by the Natural Sciences and Engineering Research Council (NSERC) of Canada Discovery Grants (VC, KB), the Canadian Foundation for Innovation Leaders Opportunity Fund (VC), the University of Waterloo Propel Centre Grant (VC, KB), the University of Waterloo CIHR Research Incentive Fund (KB), the Joseph Ellis Family Glaucoma Research Fund (KMJ) and William Black Glaucoma Research Fund (KMJ), NIH 5P30EY008126-27 to Vanderbilt Vision Research Center (KMJ), and an Unrestricted Vanderbilt Eye Institute Departmental Grant from Research to Prevent Blindness, Inc., N.Y. (KMJ). Funding sources had no involvement in: the study design, collection, analysis and interpretation of data, the writing of the report and the decision to submit the article.

Conflict of interest: AG presented some of this work at the ARVO 2015 Meeting. VC is a co-applicant on a patent describing work supported by the NSERC Grant but not related to the subject matter. The authors certify that they have no other affiliations with or involvement in any organization or entity with any financial interest (such as honoraria; educational grants; participation in speakers' bureaus; membership, employment, consultancies, stock ownership, or other equity interest; and expert testimony or patent-licensing arrangements), or non-financial interest (such as personal or professional relationships, affiliations, knowledge or beliefs) in the subject matter or materials discussed in this manuscript.

Ethical approval: All applicable international, national, and/or institutional guidelines for the care and use of animals were followed. All procedures performed in studies involving animals were in accordance with the ethical standards of the institution or practice at which the studies were conducted. This article does not contain any studies with human participants performed by any of the authors.

± 138 μV; p = 0.0002 for both). UHR-OCT images showed backward bowing in all groups during IOP elevation, with a return to typical form about 30 minutes after IOP elevation.

Conclusion—Differences in the loop-induced responses between the strains are likely due to different inherent retinal morphology and physiology.

Keywords

intraocular pressure; electroretinography; ultrahigh-resolution optical coherence tomography; rat; Long-Evans; Brown Norway; Sprague-Dawley

INTRODUCTION

Glaucoma is the second leading cause of blindness in the world [1]. It is characterized by changes in the shape of the optic nerve head (ONH), thinning of the nerve fiber layer (NFL) and abnormal function and eventual death of retinal ganglion cells (RGCs) [2]. The progressive cellular degeneration of the ganglion cell axons and retinal cells can lead to significant vision loss and blindness [2]. Currently, the absence of a cure for glaucoma requires patient monitoring for early symptoms and risk factors associated with the disease. A major risk factor of glaucoma is elevated intraocular pressure (IOP) [3]. Typical IOP in humans ranges between 10 – 21 mmHg while elevated pressure leads to optic nerve damage and resulting visual field loss [3]. Fluctuations in IOP have been described during different activities, and time of day [4–6]. Patients who experience diurnal fluctuations rather than maintaining elevated IOPs can develop glaucoma, indicating that acute short-term elevations have physiological consequences [6,7].

Although many groups have attempted to emulate the elevated IOPs in animal models to determine the functional changes leading to vision impairment [8–10], few have identified what effects fluctuating IOPs have on glaucoma development. Joos *et al.* [11] showed that intermittent short-term elevations in IOP (35.3 ± 2.6 mmHg) in Sprague Dawley rat eyes resulted in morphological changes to the structure of the retina and optic nerve. Choh *et al.* [12] used a similar model to investigate the short term changes to the retina using electroretinography and optical coherence tomography. Although electroretinography is commonly used to assess the activity of photoreceptors, bipolar cells and their outputs [13], Bui and Fortune [14] revealed that the scotopic threshold response (STR) of the electroretinogram (ERG) could be used to assess ganglion cell function in Brown Norway rats following optic nerve transection (ONT). However, Alarcon-Martinez *et al.* [15] found that STRs differed between albino and pigmented rats after ONT [15]. Moreover, in laser-induced OHT models, RGC loss was more severe in albino than in pigmented mice [16,17]. Albino mice have also shown to differ in scleral biomechanical behavior in a chronic glaucoma model [18]. Outflow facility has also been shown to differ between albino and pigmented mice [19] and the IOP-lowering effect of isoflurane anesthesia also varies among mice strains [19]. Although albino rats are often used as the model organism for studies related to RGC injury and glaucoma, differences between strains are apparent and may be useful to better understand observed effects within an experimental model.

Given that albino and pigmented rat strains demonstrate varying degrees of susceptibility to IOP elevation, this study aimed to compare the effect of acute and reversible IOP elevation on retinal function and morphology in one albino and two pigmented strains of rats.

METHODS

All procedures were conducted in accordance with the Canadian Council on Animal Care, the University of Waterloo Animal Care Committee and the ARVO statement for the use of animals in research. Eleven-week-old male Long-Evans (LE), Brown Norway (BN) and Sprague-Dawley (SD) rats (n = 5, for each group) were obtained from Harlan Labs (Indianapolis, Indiana). The rats were fed *ad libitum*, and subjected to 12-hour light-dark cycles with crepuscular periods (maximum 257 lux for 3.5 hours a day) in the housing facility. The animals were anesthetized nasally with 1.5% isoflurane during collection of the data. Each eye was provided a drop of a topical anesthetic (0.5% proparacaine hydrochloride, Alcaine: #1001600, Alcon, Mississauga, ON, Canada) followed by a pupillary dilator (0.5% tropicamide, mydriacyl, #1001600, Alcon, Mississauga, ON, Canada). Throughout the duration of an experimental procedure artificial tears (Refresh® Celluvisc® drops, Allergan, Parsippany, NJ) were administered to the rat corneas to maintain hydration. Experimental procedures were performed on the same rat on four separate days (Day 1 = STR, Day 3= ERG, Day 5 = UHR-OCT, Day 6 = Perfusion) as described in Figure 1.

Raising Intraocular Pressure

IOP measurements were made using a rebound tonometer (Icare® Tonolab, Icare Finland Oy, Helsinki, Finland). IOPs were measured for each eye before intraocular pressure was raised via a vascular loop, following the procedures outlined by Joos *et al.* [11]. The vascular loop was placed around the right eye of each rat for one hour; the loop diameter was adjusted to achieve an IOP of ~35 mmHg. The left eye was untreated to provide a control. IOP measurements were recorded from each eye 45 minutes into the loop-induced IOP elevations and then again 30 min after the removal of the loop (Figure 1).

Electrophysiology

Before electrophysiological testing on day 1, animals were dark adapted for at least 12 hours. All preparations were done under red illumination (631 nm, <10.9 lux). Scotopic threshold responses to a luminance series of weak flashes and electroretinograms to a stronger luminance series, were performed for each rat strain in separate experimental sessions. STRs were recorded using a pair of full-field flash stimulators (D213 Colorburst, Diagnosys LLC, Lowell, MA) while ERGs were recorded using a custom visual stimulator, integrated with the UHR-OCT retinal imaging probe. Both stimulus systems were connected to and controlled by a commercial ERG recording system (Espion E2, Diagnosys LLC). Electrophysiological measurements were made for both eyes before the placement of the loop, 45 minutes after the loop had been placed onto the right eye (IOP ~35 mm Hg) and 30 minutes after the loop had been removed. For both STRs and ERGs, a corneal loop electrode was placed on the corneal surface of the eye(s) while ground electrodes were placed behind the ears and in the middle of the head. For the STR recordings, the rats were dark adapted

for an additional 10 min before exposure to binocular stimuli consisting of 40 white light flashes of 4 ms duration, separated by 2-second dark intervals as per Bui and Fortune [14]. Each luminance step increased by 0.2 log steps from −6.64 log cd·s/m^2 to a maximum intensity of −3.04 log cd·s/m^2. STR amplitudes were and implicit times were analyzed for all luminance levels where a response above noise level was detected. Positive STR (pSTR) amplitudes were measured from the pre-stimulus baseline to the maximum voltage. Positive STR implicit times were measured from the onset of the stimulus flash to the peak pSTR amplitude.

On day 3, baseline ERGs were collected monocularly from the future control eye, followed by baseline recordings of the future treated eye. IOP was then raised in the treated eye and an ERG was collected 45 minutes after IOP elevation began from that eye. An ERG recording was acquired from the control eye immediately thereafter, while the loop remained on the treated eye. The loop was removed from the treated eye after it had been on for one hour. 30 minutes after removal of the loop, an ERG was recorded for the control eye followed by the treated eye. ERG stimuli consisted of 5 white light flashes (white light-emitting diode), each at 3.73 cd·s/m^2 for 7 ms, separated by 1 min dark intervals. ERG data were acquired for 1 second including a 10 ms baseline recording before the flashes. ERG a-wave amplitudes were measured as the absolute value of the maximum trough of the a-wave from the baseline voltage. ERG a-wave implicit times were measured from the onset of the stimulus to the maximum trough of the a-wave. ERG b-wave amplitudes were measured from the trough of the a-wave to the maximum peak of the b-wave. ERG b-wave implicit times were measured from the onset of the stimulus to the maximum peak of the b-wave. Oscillatory potentials (OPs) were isolated from ERG recordings using a customized SigmaPlot bandpass filter (100–300 Hz). OP amplitudes were calculated by taking the average of the OP peak difference between the preceding and following troughs. Implicit times for the OPs were measured from the onset of the stimulus to the OP peak. OP amplitudes and implicit times were measured for five OPs.

Ultrahigh-resolution Optical Coherence Tomography (UHR-OCT)

Two-dimensional (2D) cross sectional images of the rat retina were acquired using a research grade UHR-OCT system [12]. The system uses a broadband superluminescent diode (Superlum Ltd., λ_c = 1020 nm, $\Delta\lambda$= 110 nm, Pout = 10 mW) for a light source, and provides axial resolution of 3 μm and lateral resolution of ~5μm in retinal tissue. The OCT data were acquired with a 1024 pixel InGaAs camera (SUI, UTC Aerospace Systems) interfaced with a custom-built OCT spectrometer (P&P Optica Inc.) at the rate of 47,000 lines/second. The UHR-OCT system provided ~105 dB SNR for 1.7 mW optical imaging power incident on the cornea. On day 5, all images were acquired for both eyes, before the placement of the loop, 45 minutes after the loop had been placed onto the OD (IOP ~35 mm Hg), and 30 minutes after the loop had been removed. Volumetric UHR-OCT images (1000 frames × 1000 lines/frame × 1024 pixels/line) of the rat retinas were acquired from a region in the rat eye centered at the optic nerve head (ONH) from an area of approximately 2 mm^2. Cross sectional images (3000 lines/frame × 1024 pixels/line) of the retina were also acquired from a circular scan around the optic nerve head at a radial distance of ~0.7 mm away from the center of the ONH. All UHR-OCT images were acquired monocularly in the same

relative order mentioned above for the ERGs. All retinal UHR-OCT images were dispersion compensated numerically following a similar approach to the one developed by Wojtkowski *et al.* [20]. A custom semi-automatic MATLAB® (Natick, Massachusetts) algorithm developed by our research group was used to determine the nerve fiber layer (NFL), ganglion cell layer (GCL) and inner plexiform layer (IPL) layer thicknesses [21]. Blood vessels were ignored while determining layer thicknesses. The thickness for these layers were summed to provide the ganglion cell complex (GCC) thickness. Additionally, the total retinal thickness was measured and defined as the distance between the NFL and the retinal pigment epithelial layer (RPE). Volumetric images were generated using Amira® (Hillsboro, Oregon) and used to compare overall structural changes to the rat retinas associated with the acutely elevated IOP. The change in cross sectional depth of the Bruch's membrane opening (xBMO), defined as the point at which the Bruch's membrane (BM)/RPE interface ends on either side of the optic nerve head in a cross-sectional OCT image, was calculated using the B-scan containing the center of the optic nerve head. The center B-scan of the optic nerve head was determined by finding the center scan of an ellipse fit to the 2D *en face* projection of the 3D stack. Each xBMO depth was determined by connecting the BM/RPE interfaces at the furthest edges of the image (reference plane) and calculating the shortest distance from the xBMO to the reference plane [12].

Histology and Immunocytochemistry

One day after the last IOP elevation (five days after the initial IOP elevation), the rats were anaesthetized with isoflurane until they were unresponsive to toe pinches. Rats underwent cardiac perfusion with saline followed by 4% (w/v) paraformaldehyde in phosphate buffered saline (PBS). Eyes were enucleated and a suture was placed at the nasal limbus to mark the orientation of the eye. Globes were post-fixed for two days in 4% (w/v) paraformaldehyde in PBS then briefly stored in PBS. Graded alcohol and acetone were used to dehydrate the globes, which were then embedded in paraffin. Eyes were sectioned and retinal sections were treated for antigen retrieval prior to blocking as previously described [12]. Rabbit monoclonal anti-microtubule-associated protein 1A/1B-light chain 3 (LC3) antibodies (anti-LC3A/B (N-term); 1:100; #MABC176, Millipore, Billerica, MA) was used as a primary antibody to evaluate for autophagy. Sections were labelled with primary antibodies overnight at 4 °C before incubation with rhodamine-conjugated goat anti-rabbit IgG antibodies for LC3. Negative controls were stained without the use of a primary antibody. Slides were analyzed using a Zeiss Confocal Microscope (LSM 510 Meta, Zeiss, Germany).

Statistical Analysis

All statistical tests were carried out using STATISTICA Version 10 (Statsoft, Boston, MA). Results were considered to be significant if $p < 0.05$. For electrophysiological data, a mixed-model analysis of variance (ANOVA) was used to determine differences in amplitudes and implicit times, with the eye (treated or control) and loop condition (pre-, during, and post-loop wear) as the dependent factors, and rat strain (SD, LE and BN) as the independent factor. For morphological thickness data, the same tests were carried out to compare difference in retinal layer thicknesses, with the eye and rat strain as dependent and independent factors, respectively. Post-hoc dependent data were analyzed using Bonferroni-

corrected multiple comparison tests, while independent data were analyzed using Tukey's test. Greenhouse-Geisser corrections were used where epsilon values were <0.75.

RESULTS

Strain-dependent differences were not observed for IOPs for the STR and ERG protocols ($p = 0.1763$ and $p = 0.1640$, respectively). A strain-dependent difference was observed for UHR-OCT experiments ($p=0.0258$), with the IOPs for LE rats greater than both the BN ($p=0.0013$) and SD ($p=0.0002$; Table 1).

Electroretinography

During IOP elevation, all rat strains exhibited increases in positive STR responses with a recovering response after IOP release (Figure 2). However, analysis of pSTR amplitudes, for LE and BN rats, revealed a relatively greater response to acute IOP elevation (Figure 2B). When comparing response amplitudes, for all three strains, during IOP elevation, LE (mean ± standard deviation: 259 ± 124 μV) and BN (228 ± 96 μV) rats had significantly higher responses compared to SD (56 ± 46 μV) rats ($p = 0.0002$ for both; Figure 2C). These differences were only apparent while IOP was elevated as both treated and control eyes, pre- and post-loop, showed no significant differences ($p > 0.9928$). Moreover, in conjunction with larger amplitudes, pSTR implicit times for LE rats were significantly shorter than in the BN and SD rats ($p = 0.0300$ and $p = 0.0250$, respectively; Figure 2C inset).

Similar to the pSTR data, ERG recordings for all three rat strains illustrated larger b-wave and a-wave amplitudes during elevated IOP (Figure 3A). However, b-wave amplitudes were 2-fold higher in LE and BN rats compared to SD rats (947 ± 129μV & 892 ± 184 μV, vs 427 ± 138 μV; $p = 0.0002$ for both; Figure 3C). SD rats had larger overall b-wave implicit times compared to either LE or BN rats ($p = 0.0090$ and $p = 0.0080$, respectively). Moreover, a-wave amplitudes during elevated IOP in LE and BN rats were about 1.5 and 1.9 fold higher than in SD rats (376 ± 30 μV and 468 ± 51 μV vs 242 ± 107 μV; $p = 0.0008$ & $p = 0.0002$, respectively; Figure 3B). Similarly to b-wave implicit times, a-wave implicit times also showed a significant difference between SD and both LE and BN rats ($p = 0.0002$ and $p = 0.0006$, respectively).

Oscillatory potential amplitudes for each of the three strains responded uniquely to elevated IOP (Figure 4). For LE rats, during IOP elevation, OP2 and OP3 were each significantly larger than their respective pre- and post-loop conditions ($p < 0.0004$ for both), while OP1, 4 and 5 did not significantly change in response to elevated IOP ($p = 1.0000$). Unlike LE rats, only OP2 increased significantly in BN rats, during IOP elevation ($p < 0.0001$) while OP1, 3, 4 and 5 did not change ($p > 0.1179$). For SD rats, only OP3 significantly increased during IOP elevation ($p > 0.0452$) while the others did not change ($p >0.9438$). IOP elevation also resulted in changes to the implicit times of specific OPs for each strain.

For all strains, control eye implicit times did not change as a function of the loop condition ($p > 0.0823$). For LE rats, IOP-elevated eyes showed longer OP3 implicit times compared to the post-loop ($p = 0.0094$) but not to pre-loop ($p = 0.0823$) conditions, and these implicit times were also not different from control eyes at the same time point ($p = 0.0823$). OP4

implicit times in treated eyes were longer during loop-wear than during both pre- ($p = 0.0021$) and post- ($p = 0.0004$) loop conditions and the control eye at the same time point ($p = 0.0002$). For IOP-elevated eyes in BN rats, all OP implicit times were longer compared to their respective pre- or post-loop conditions ($p < 0.0406$), and to their control eyes at the same time point ($p<0.0009$). For SD rats, during IOP elevation, treated eye OP3 implicit times were longer than their respective pre-loop ($p < 0.0001$) but not post-loop ($p = 1.0000$) conditions, while OP4 and OP5 were also longer during elevated IOP than compared to the pre- and post-loop conditions ($p < 0.0148$). For all three OPs, treated eye implicit times during IOP elevation were longer than in the control eyes at the same time points ($p>0.0009$). For all strains, pre- and post-loop condition implicit times were not different between treated and control eyes ($p > 0.1052$).

Strain-dependent differences in amplitudes were not observed for OP1, OP4 and OP5 ($p > 0.1996$) across all loop conditions (Table 2). Differences were observed for OP2 amplitudes, with both LE and BN rats showing significantly higher amplitudes than those for SD rats across all loop conditions ($p < 0.0003$). LE and BN amplitudes for this OP were not different across all loop conditions ($p > 0.2019$). OP3 amplitude patterns were similar for all loop conditions (cf. LE & BN vs SD: $p < 0.0002$; LE vs BN: $p > 0.9999$) except for the pre-loop condition, where BN rat amplitudes were higher than those for both LE and SD rats ($p < 0.0027$), the latter two of which were not different ($p=0.1467$).

During IOP elevation, only OP5 implicit times were different amongst the strains, with treated eye implicit times longer for BN rats than LE ($p=0.0047$) and SD rats ($p=0.0497$), and the latter two implicit times not different ($p=0.9999$). Strain-dependent differences were not observed for the treated eye implicit times in the pre- and post-loop conditions ($p > 0.8912$), nor were they observed for control eyes for all loop conditions ($p > 0.8206$).

Ultrahigh-resolution Optical Coherence Tomography and Immunohistochemistry

The cross-sectional and volumetric images revealed large qualitative changes to the retinal structure during IOP elevation (Figure 5). For all three strains, IOP elevation using the vascular loop method appeared to have caused characteristic backward bowing of the optic nerve head [22,23]. Analysis of the baseline GCC layer thickness revealed significant differences between each rat strain at baseline. Accordingly, LE rats have the thickest GCC followed by BN and SD rats ($p = 0.0051$ for LE vs BN, $p = 0.0002$ for LE vs SD, and $p = 0.0051$ for BN vs SD; Figure 6). However, LE rats had the thickest retinas than compared to BN or SD rats ($p = 0.0454$ for LE vs BN, $p = 0.0280$ for LE vs SD; Table 3), while BN and SD rat retinal thicknesses did not significantly differ ($p = 0.9599$; Table 3). For all three strains, the xBMO in the treated eye was significantly deeper during IOP elevation (133 ± 26 μm) than compared to the pre- (75 ± 32 μm, $p < 0.0002$) and post-loop (70 ± 22 μm, $p < 0.0001$) conditions (Figure 7B). The xBMO in the control eye did not change with respect to the loop conditions ($p = 1.0000$). The xBMO depth in response to IOP elevation did not depend on the strain of rat ($p = 0.2786$), despite the significantly higher IOP in the LE rats (Table 1). LC3 expression was present in both LE and BN treated and control retinas (Figure 8).

DISCUSSION

Similar baseline scotopic ERG recordings for albino and pigmented rats have been reported previously by Alarcon-Martinez *et al.* [15] and Polosa *et al.* [24], although not all authors agree. Lezmi *et al.*, [25] showed that b-wave amplitudes in BN were greater than those in SD rats. The differences in the findings amongst the studies might be related to the anaesthetics used and sample size; Alarcon-Martinez *et al.* [15] used ketamine:xylazine and 31 SD vs 24 Piebald-Viral-Glaxo pigmented rats, Lezmi *et al.* [25] used Imalgen:Domitor as their anaesthetic and 12 SD and 12 BN rats, and we used isoflurane and 5 rats each for the 3 strains. Except for the anaesthetic used (ketamine:xylazine), Polosa *et al.* [24] used the same strains we did at 12 animals per strain, and with an additional albino Lewis Wistar strain. The combination of the different strains, sample sizes and anaesthetic used could all contribute to the disparate results between these 4 studies.

A treatment-associated strain difference was also observed in this study, with pigmented rats showing greater responses to moderate IOP-elevation; it is likely that the these strain differences, whether arising from variations in genetic background or pigmentation, govern the physiological responses to the intervention. Although the treatment is different, differences between the albino and pigmented strains were also found in the recovery response of the ERG after axotomy [15], indicating that treatment-associated strain differences were present.

Albino rats have no melanin in their eyes, specifically in their iris and pigment epithelial layer of the retina and their retinas have fewer rod photoreceptors and retinal ganglion cells making it difficult to detect low-level light such as the stimuli used in STRs [26,27], although the number of photoreceptors, estimated by outer nuclear layer thickness, does not differ amongst the strains [28,29]. The neural connections between the eyes and the brain in albino rats also have been found to be abnormal, contributing to their poor vision [30] and it is known that there are cytoarchitectural differences between albino and pigmented strains in the neurons that are involved with circadian rhythms [31,32]. Although we did not observe a difference in IOP levels between the strains (Table 1), IOP levels are influenced by circadian rhythms [16,33]; thus it is possible that IOP-related strain differences were influenced by strain-dependent circadian rhythms. Albino Wistar rats have demonstrated greater susceptibility to ischaemic damage from elevated IOP (35 min, 120 mmHg), indicated by significant decreases in ERG b-wave amplitudes that did not occur in pigmented rats [34] and albino rabbit retinas have also demonstrated a failure to recover b-wave ERG amplitudes after 2 hours of ischemia, unlike pigmented rabbits, which exhibited total ERG recovery [35]; STR and ERG amplitudes in the albino rats of the present study appear to be consistent with the general relative suppression of the ERG responses to IOP elevations. Although the data should be interpreted cautiously, we note that LE rats, which are bred from a pigmented (wild grey) and an albino (Wistar) rat, showed IOP-associated changes in OP2 and OP3 amplitudes that were also observed individually for the pigmented (OP2) and albino (OP3) rats, respectively. These data may suggest a OP component-specific vulnerability to IOP elevation, which also has been shown in humans to differ in response to transient changes in retinal vascular perfusion pressure [36]. It should be noted that not all differences observed between the strains is related to the amount of pigmentation. The genetic background of the

animals likely plays a role. Polosa *et al.* [24] showed pigmented BN and albino SD albino rats were more affected by light-induced damage than pigmented LE and albino Lewis Wistar rats, while the LaVail *et al.* [37] showed differential light-induced damage on two different strains of albino mice.

Tan *et al.* [38] showed that the thickness of the GCC is a sensitive marker for identifying glaucomatous eyes [38–40]. In our study, we have demonstrated that GCC thickness differs significantly between each of the rat strains, while the total retinal thickness for LE rats differed from BN and SD rats, suggesting that differences in GCC thicknesses between rats could play a role in the response to factors that are associated with the IOP-induced enhancement. GCCs for our BN rats (Table 3) are slightly thinner than those reported by Lozano and Twa[41], who reported values between 65 ± 5 to 73 ± 5 μm for approximately the same scanning region. Lozano and Twa[41], used a horizontal linear scan, therefore limiting retinal thicknesses in either a superior or inferior hemi-field, while we averaged the thicknesses from a circular scan, thereby including regions of varying thicknesses for all 4 quadrants of the retina. Elevated IOP was found to cause changes in the shape of the optic nerve head, characterized as a bowing of the retina. Similarly, others have demonstrated backward bowing of the lamina cribrosa during elevated IOP [42] and in glaucomatous eyes [43] suggesting that changes to the structure we observed are IOP related and not a result of the vascular loop model.

Although a lower number of animals were used in the present study, the responses to the IOP elevations in all the rats were consistent with previous work using the same IOP elevation model in SD rats [12]. Potential mechanisms responsible for the large increase in retinal responses, that occurred for all three strains during IOP elevation, have been discussed in a previous paper by our group [12]. Specifically, a study by Ward *et al.* [44] demonstrated an increase in excitatory signals in RGCs in response to IOP elevation using the microbead injection model. Their results were attributed to increased retinal activity as a result of IOP-induced stress on the vanilloid family of cation channels. Enhanced pSTRs observed in our study may be related to a similar mechanism. Moreover, nitric oxide (NO), which is associated with chronic IOP elevation, has shown to contribute to increased STR and ERG a- and b-wave amplitudes [45]. The enhancements of the ERG and STR amplitudes were about 2-fold in the study by Vielma *et al.* [45]; factors that might account for the larger enhancement observed in the present study include the observation that NO was injected rather than putatively produced from IOP elevations, and the anaesthetic used. STR data from our group (Choh *et al.*, manuscript under review) show that the fold increase in ketamine:xylazine-anaesthetised rats with acute moderate elevations of IOPs is also at about 2-fold. These mechanisms may vary between strains of rat; NO levels in pigmented Piebald-Virol-Glaxo rats are higher than in albino Lewis rats in experimental autoimmune encephalomyelitis models [46], and intravitreal injections of NO donors led to damaged retinas in albino but not in pigmented rabbits [47–49]. The mechanisms underlying strain-differences are certainly a topic that requires further investigation.

LC3 has been shown to be a marker for autophagy as it associated with autophagosomes and autolysosomes [50]. An increase in LC3 expression has also been reported in chronic glaucoma models as a result of autophagosome accumulation in dendrites and cytoplasm of

retinal ganglion cells after IOP elevation [51]. LC3 expression as a result of acute IOP elevation was not different for LE and BN treated and control eyes, indicating that a non-pathological effect. These results are consistent with our previous experiment on SD rats with acutely raised IOPs [12], which also indicated no difference in LC3 expression between treated and control eyes [12]. Together, the two studies indicate that acute IOPs elevation does not differentially affect LC3 expression. It is important to note that the experiments carried out in this study were acute. Chronic models may reveal differential LC3 expression as a result of unique levels of susceptibility to elevated IOP.

In summary, these results indicate that LE and BN rats have greater electrophysiologic responses to acute, moderately elevated IOP than compared to SD rats. All three strains exhibited larger ERG amplitudes during acute moderately elevated IOP. Moreover, GCC complex thicknesses differ significantly between rat strains with LE having the greatest thickness followed by BN and SD rats. xBMO depth increased during IOP elevation. Lastly, LC3 expression did not differ between strains or treated and control eyes. Intrinsic morphological differences between rat strains are associated with unique responses to elevated IOP. Understanding how these morphological characteristics are related to the effects of moderately elevated IOP may further our understanding of its risk and association with glaucoma. The observation of strain differences not only among albino and pigmented, but also between the two pigmented strains, indicate that potential strain differences should be considered when choosing an animal model.

Acknowledgments

The authors would like to thank Nancy Gibson for assistance with the animal handling and housing. Thank you to Daphne McCulloch for her helpful comments and criticisms of the manuscript. We would also like to thank Camillo Correa Ochoa, and Kirstie Carter for their assistance with the animal experiments and processing of the UHR-OCT images. Additionally, we would like to thank Ratna Prasad at the Vanderbilt Eye Institute for processing the immunohistochemistry slides. This work was funded in part by the Natural Sciences and Engineering Research Council (NSERC) of Canada Discovery Grants (VC, KB), the Canadian Foundation for Innovation Leaders Opportunity Fund (VC), the University of Waterloo Propel Centre Grant (VC, KB, KMJ), the University of Waterloo CIHR Research Incentive Fund (KB, VC, KMJ), the Joseph Ellis Family Glaucoma Research Fund (KMJ) and William Black Glaucoma Research Fund (KMJ), NIH 5P30EY008126-27 to Vanderbilt Vision Research Center (KMJ), and an Unrestricted Vanderbilt Eye Institute Departmental Grant from Research to Prevent Blindness, Inc., N.Y. (KMJ).

References

1. Kingman S. Glaucoma is second leading cause of blindness globally. Bull World Health Organ. 2004; 82(11):887–888. [PubMed: 15640929]
2. Quigley HA, Nickells RW, Kerrigan LA, Pease ME, Thibault DJ, Zack DJ. Retinal ganglion cell death in experimental glaucoma and after axotomy occurs by apoptosis. Invest Ophthalmol Vis Sci. 1995; 36(5):774–786. [PubMed: 7706025]
3. Lee DA, Higginbotham EJ. Glaucoma and its treatment: a review. Am J Health Syst Pharm. 2005; 62(7):691–699. [PubMed: 15790795]
4. Carlson KH, McLaren JW, Topper JE, Brubaker RF. Effect of body position on intraocular pressure and aqueous flow. Invest Ophthalmol Vis Sci. 1987; 28(8):1346–1352. [PubMed: 3610552]
5. Weinreb RN, Cook J, Friberg TR. Effect of inverted body position on intraocular pressure. Am J Ophthalmol. 1984; 98(6):784–787. [PubMed: 6507552]
6. Drance SM. The significance of the diurnal tension variations in normal and glaucomatous eyes. Arch Ophthalmol. 1960; 64:494–501. [PubMed: 13724271]

7. Asrani S, Zeimer R, Wilensky J, Gieser D, Vitale S, Lindenmuth K. Large diurnal fluctuations in intraocular pressure are an independent risk factor in patients with glaucoma. J Glaucoma. 2000; 9(2):134–142. [PubMed: 10782622]
8. Frankfort BJ, Khan AK, Tse DY, Chung I, Pang J-J, Yang Z, Gross RL, Wu SM. Elevated intraocular pressure causes inner retinal dysfunction before cell loss in a mouse model of experimental glaucoma. Invest Ophthalmol Vis Sci. 2013; 54(1):762–770. [PubMed: 23221072]
9. Fortune B, Bui BV, Morrison JC, Johnson EC, Dong J, Cepurna WO, Jia L, Barber S, Cioffi. Selective Ganglion Cell Functional Loss in Rats with Experimental Glaucoma. Invest Ophthalmol Vis Sci. 2004; 45(6):1854–1862. [PubMed: 15161850]
10. Mittag TW, Danias J, Pohorenec G, Yuan HM, Burakgazi E, Chalmers-Redman R, Podos SM, Tatton WG. Retinal damage after 3 to 4 months of elevated intraocular pressure in a rat glaucoma model. Invest Ophthalmol Vis Sci. 2000; 41(11):3451–3459. [PubMed: 11006238]
11. Joos KM, Li C, Sappington RM. Morphometric Changes in the Rat Optic Nerve Following Short-term Intermittent Elevations in Intraocular Pressure. Invest Ophthalmol Vis Sci. 2010; 51(12): 6431–6440. [PubMed: 20688743]
12. Choh V, Gurdita A, Tan B, Prasad RC, Bizheva K, Joos KM. Short-term moderately intraocular pressure is associated with elevated scotopic electroretinogram responses. Invest Ophthalmol Vis Sci. 2016; 57(4):2140–2151. [PubMed: 27100161]
13. Pinilla I, Lund RD, Sauvé Y. Contribution of rod and cone pathways to the dark-adapted electroretinogram (ERG) b-wave following retinal degeneration in RCS rats. Vision Res. 2004; 44(21):2467–2474. [PubMed: 15358082]
14. Bui BV, Fortune B. Ganglion cell contributions to the rat full-field electroretinogram. J Physiol (Lond). 2004; 555(Pt 1):153–173. [PubMed: 14578484]
15. Alarcon-Martinez L, de la Villa P, Aviles-Trigueros M, Blanco R, Villegas-Perez MP, Vidal-Sanz M. Short and long term axotomy-induced ERG changes in albino and pigmented rats. Mol Vis. 2009; 15(November):2373–2383. [PubMed: 19936311]
16. Valiente-Soriano FJ, Salinas-Navarro M, Jimenez-Lopez M, Alarcon-Martinez L, Ortin-Martinez A, Bernal-Garro JM, Aviles-Trigueros M, Agudo-Barriuso M, Villegas-Perez MP, Vidal-Sanz M. Effects of ocular hypertension in the visual system of pigmented mice. PLoS ONE. 2015; 10(3):e0121134. [PubMed: 25811653]
17. Cone FE, Steinhart MR, Oglesby EN, Kalesnykas G, Pease ME, Quigley HA. The effects of anesthesia, mouse strain and age on intraocular pressure and an improved murine model of experimental glaucoma. Exp Eye Res. 2012; 99:27–35. [PubMed: 22554836]
18. Nguyen C, Cone FE, Nguyen TD, Coudrillier B, Pease ME, Steinhart MR, Oglesby EN, Jefferys JL, Quigley HA. Studies of scleral biomechanical behavior related to susceptibility for retinal ganglion cell loss in experimental mouse glaucoma. Invest Ophthalmol Vis Sci. 2013; 54(3):1767–1780. [PubMed: 23404116]
19. Boussommier-Calleja A, Overby DR. The influence of genetic background on conventional outflow facility in mice. Invest Ophthalmol Vis Sci. 2013; 54(13):8251–8258. [PubMed: 24235015]
20. Wojtkowski M, Srinivasan V, Ko T, Fujimoto J, Kowalczyk A, Duker J. Ultrahigh-resolution, high-speed, Fourier domain optical coherence tomography and methods for dispersion compensation. Opt Express. 2004; 12(11):2404–2422. [PubMed: 19475077]
21. Mishra A, Wong A, Bizheva K, Clausi DA. Intra-retinal layer segmentation in optical coherence tomography images. Optics Express. 2009; 17(26):23719–23728. [PubMed: 20052083]
22. Fortune B, Yang H, Strouthidis NG, Cull GA, Grimm JL, Downs JC, Burgoyne CF. The effect of acute intraocular pressure elevation on peripapillary retinal thickness, retinal nerve fiber layer thickness, and retardance. Invest Ophthalmol Vis Sci. 2009; 50(10):4719–4726. [PubMed: 19420342]
23. Quigley HA. The pathogenesis of reversible cupping in congenital glaucoma. Am J Ophthalmol. 1977; 84(3):358–370. [PubMed: 900230]
24. Polosa A, Bessaklia H, Lachapelle P. Strain Differences in Light-Induced Retinopathy. PLoS ONE. 2016; 11(6):e0158082. [PubMed: 27355622]

25. Lezmi S, Rokh N, Saint-Macary G, Pino M, Sallez V, Thevenard F, Roome N, Rosolen S. Chloroquine causes similar electroretinogram modifications, neuronal phospholipidosis and marked impairment of synaptic vesicle transport in albino and pigmented rats. Toxicology. 2013; 308:50–59. [PubMed: 23567313]
26. Grant S, Patel NN, Philp AR, Grey CN, Lucas RD, Foster RG, Bowmaker JK, Jeffery G. Rod photopigment deficits in albinos are specific to mammals and arise during retinal development. Vis Neurosci. 2001; 18(2):245–251. [PubMed: 11417799]
27. Nadal-Nicolas FM, Salinas-Navarro M, Jimenez-Lopez M, Sobrado-Calvo P, Villegas-Perez MP, Vidal-Sanz M, Agudo-Barriuso M. Displaced retinal ganglion cells in albino and pigmented rats. Front Neuroanat. 2014; 8:99–99. [PubMed: 25339868]
28. Peters S, Lamah T, Kokkinou D, Bartz-Schmidt KU, Schraermeyer U. Melanin protects choroidal blood vessels against light toxicity. Z Naturforsch C. 2006; 61(5–6):427–433. [PubMed: 16869503]
29. Rapp LM, Smith SC. Evidence against melanin as the mediator of retinal phototoxicity by short-wavelength light. Exp Eye Res. 1992; 54(1):55–62. [PubMed: 1541341]
30. Taylor AM, Jeffery G, Lieberman AR. Subcortical afferent and efferent connections of the superior colliculus in the rat and comparisons between albino and pigmented strains. Exp Brain Res. 1986; 62(1):131–142. [PubMed: 3956628]
31. Valiente-Soriano FJ, Garcia-Ayuso D, Ortin-Martinez A, Jimenez-Lopez M, Galindo-Romero C, Villegas-Perez MP, Agudo-Barriuso M, Vugler AA, Vidal-Sanz M. Distribution of melanopsin positive neurons in pigmented and albino mice: evidence for melanopsin interneurons in the mouse retina. Front Neuroanat. 2014; 8:131. [PubMed: 25477787]
32. Steininger TL, Rye DB, Gilliland MA, Wainer BH, Benca RM. Differences in the retinohypothalamic tract in albino Lewis versus brown Norway rat strains. Neuroscience. 1993; 54(1):11–14. [PubMed: 8390623]
33. Drouyer E, Dkhissi-Benyahya O, Chiquet C, WoldeMussie E, Ruiz G, Wheeler LA, Denis P, Cooper HM. Glaucoma alters the circadian timing system. PLoS ONE. 2008; 3(12):e3931. [PubMed: 19079596]
34. Safa R, Osborne NN. Retinas from albino rats are more susceptible to ischaemic damage than age-matched pigmented animals. Brain Res. 2000; 862(1–2):36–42. [PubMed: 10799666]
35. Muller A, Villain M, Favreau B, Sandillon F, Privat A, Bonne C. Differential effect of ischemia/reperfusion on pigmented and albino rabbit retina. J Ocul Pharmacol Ther. 1996; 12(3):337–342. [PubMed: 8875340]
36. Kergoat H, Lovasik JV. The effects of altered retinal vascular perfusion pressure on the white flash scotopic ERG and oscillatory potentials in man. Electroencephalogr Clin Neurophysiol. 1990; 75(4):306–322. [PubMed: 1691079]
37. LaVail MM, Gorrin GM, Repaci MA, Thomas LA, Ginsberg HM. Genetic regulation of light damage to photoreceptors. Invest Ophthalmol Vis Sci. 1987; 28(7):1043–1048. [PubMed: 3596986]
38. Tan O, Li Gl, Lu AT-H, Varma R, Huang D. Mapping of macular substructures with optical coherence tomography for glaucoma diagnosis. Ophthalmology. 2008; 115(6):949–956. [PubMed: 17981334]
39. Tan O, Chopra V, Lu AT-H, Schuman JS, Ishikawa H, Wollstein G, Varma R, Huang D. Detection of macular ganglion cell loss in glaucoma by Fourier-domain optical coherence tomography. Ophthalmology. 2009; 116(12):2305–2314. [PubMed: 19744726]
40. Schulze A, Lamparter J, Pfeiffer N, Berisha F, Schmidtmann I, Hoffmann EM. Diagnostic ability of retinal ganglion cell complex, retinal nerve fiber layer, and optic nerve head measurements by Fourier-domain optical coherence tomography. Graefes Arch Clin Exp Ophthalmol. 2011; 249(7): 1039–1045. [PubMed: 21240522]
41. Lozano DC, Twa MD. Quantitative evaluation of factors influencing the repeatability of SD-OCT thickness measurements in the rat. Invest Ophthalmol Vis Sci. 2014; 53(13):8378–8385.
42. He Z, Bui BV, Vingrys AJ. The rate of functional recovery from acute IOP elevation. Invest Ophthalmol Vis Sci. 2006; 47(11):4872–4880. [PubMed: 17065501]

43. Quigley HA, Hohman RM, Addicks EM, Massof RW, Green WR. Morphologic changes in the lamina cribrosa correlated with neural loss in open-angle glaucoma. Am J Ophthalmol. 1983; 95(5):673–691. [PubMed: 6846459]
44. Ward NJ, Ho KW, Lambert WS, Weitlauf C, Calkins DJ. Absence of transient receptor potential vanilloid-1 accelerates stress-induced axonopathy in the optic projection. J Neurosci. 2014; 34(9): 3161–3170. [PubMed: 24573275]
45. Vielma A, Delgado L, Elgueta C, Osorio R, Palacios AnG, Schmachtenberg O. Nitric oxide amplifies the rat electroretinogram. Exp Eye Res. 2010; 91(5):700–709. [PubMed: 20732319]
46. Staykova MA, Cowden W, Willenborg DO. Macrophages and nitric oxide as the possible cellular and molecular basis for strain and gender differences in susceptibility to autoimmune central nervous system inflammation. Immunol Cell Biol. 2002; 80(2):188–197. [PubMed: 11940120]
47. Behar-Cohen FF, Goureau O, D'Hermies F, Courtois Y. Decreased Intraocular Pressure Induced by Nitric Oxide Donors Is Correlated to Nitrite Production in the Rabbit Eye. Invest Ophthalmol Vis Sci. 1996; 37(8):1711–1715. [PubMed: 8675417]
48. Oku H, Yamaguchi H, Sugiyama T, Kojima S, Ota M, Azuma I. Retinal toxicity of nitric oxide released by administration of a nitric oxide donor in the albino rabbit. Invest Ophthalmol Vis Sci. 1997; 38(12):2540–2544. [PubMed: 9375573]
49. Takahata K, Katsuki H, Kume T, Ito K, Tochikawa Y, Muraoka S, Yoneda F, Kashii S, Honda Y, Akaike A. Retinal neurotoxicity of nitric oxide donors with different half-life of nitric oxide release: involvement of N-methyl-D-aspartate receptor. J Pharmacol Sci. 2003; 92(4):428–432. [PubMed: 12939529]
50. Wang AL, Boulton ME, Dunn WA, Rao HV, Cai J, Lukas TJ, Neufeld AH. Using LC3 to monitor autophagy flux in the retinal pigment epithelium. Autophagy. 2009; 5(8):1190–1193. [PubMed: 19855195]
51. Park HYL, Kim JH, Park CK. Activation of autophagy induces retinal ganglion cell death in a chronic hypertensive glaucoma model. Cell Death Dis. 2012; 3:e290–e290. [PubMed: 22476098]

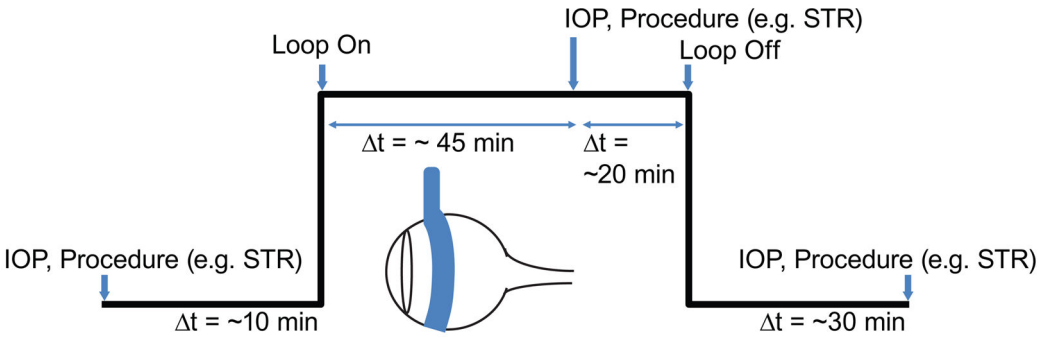

Fig. 1.

Time line for the experimental procedures. The black line reflects the protocol as a function of IOP over time for the right eye. The blue arrow-head indicates the time at which a measurement was made or the vascular loop was used. This protocol was repeated for different types of measurements (e.g. STR, ERG and UHR-OCT) on a 5-day schedule (1 day break between measurements).

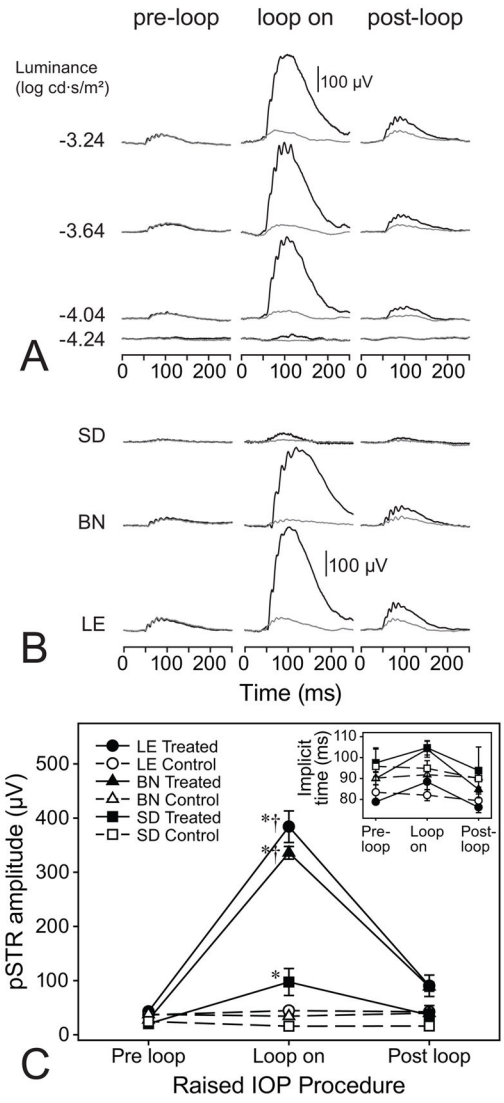

Fig. 2.

STR responses pre- during- and post-IOP elevation. (a) Representative STRs for a LE rat for both treated (black) and control (gray) eyes, pre-, during- and post-IOP elevation at multiple luminances. Flash onset is at 0 ms. (b) Representative STRs for each of the three strains at a luminance of −3.04 log cd·s/m^2. Flash onset is at 0 ms. (c) Mean pSTR amplitudes for LE, BN and SD rats at a luminance of −3.04 log cd·s/m^2. Error bars are standard error of means. The inset graph reflects mean pSTR implicit times for each rat strain, treated and control eyes and pre-, during- and post-IOP elevation. Asterisks (*) indicate differences relative to pre-loop conditions for the rat strain. Daggers (†) reflect a significant difference relative to SD rats at the same loop-condition.

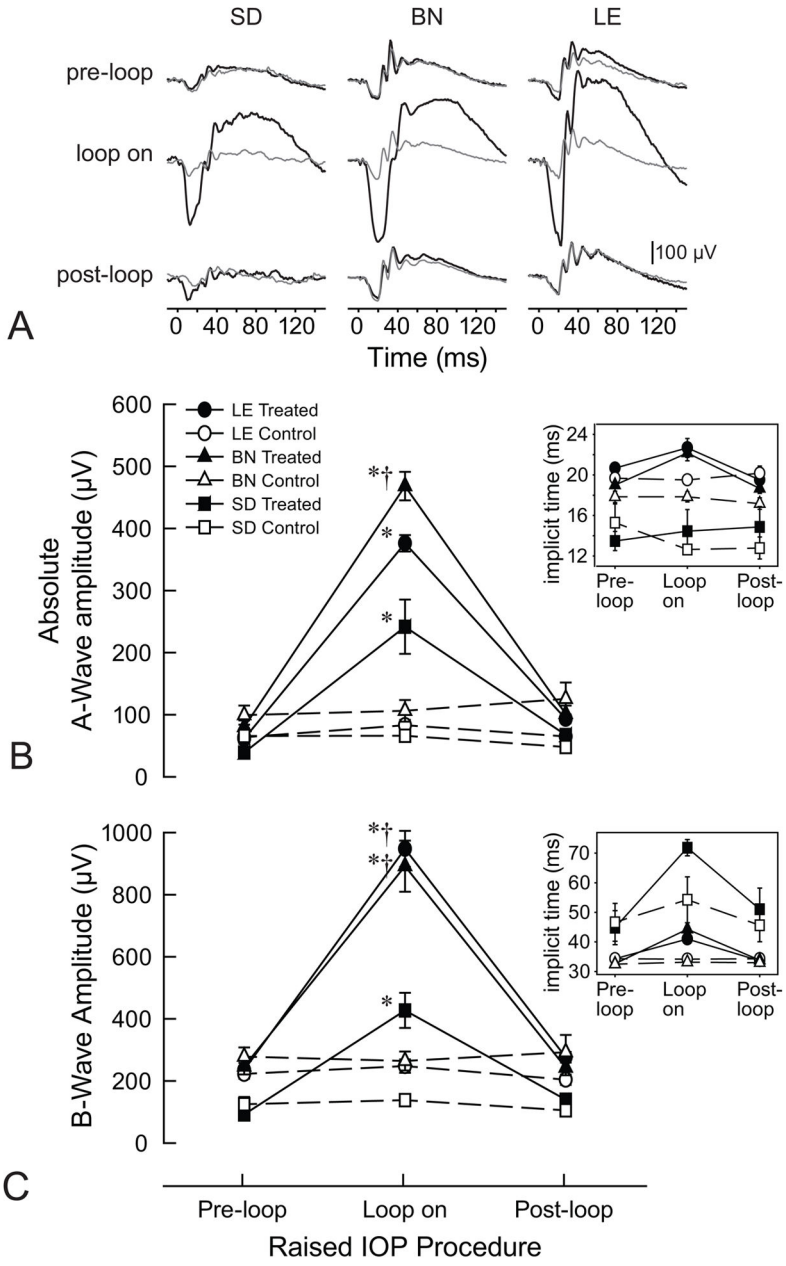

Fig. 3.

ERG responses pre- during- and post-IOP elevation. (a) Sample ERGs for SD, BN and LE rats for both treated (black) and control (gray) eyes, pre-, during- and post-IOP elevation. Flash onset is at 0 ms. (b) Mean ERG a-wave amplitudes for each rat strain, treated and control eye, and pre-, during and after-IOP elevation. Error bars are standard error of means. The inset graph reflects mean ERG a-wave implicit times for each rat strain, treated and control eyes and pre-during and post-IOP elevation. (c) Mean ERG b-wave amplitudes for each rat strain, treated and control eye, and pre-, during and post-IOP elevation. Error bars are standard error of means. The inset graph reflects mean ERG b-wave implicit times for each rat strain, treated and control eyes and pre-during and post-IOP elevation. Asterisks (*)

indicate differences relative to pre-loop conditions for the rat strain. Daggers (†) reflect a significant difference relative to SD rats at the same loop-condition.

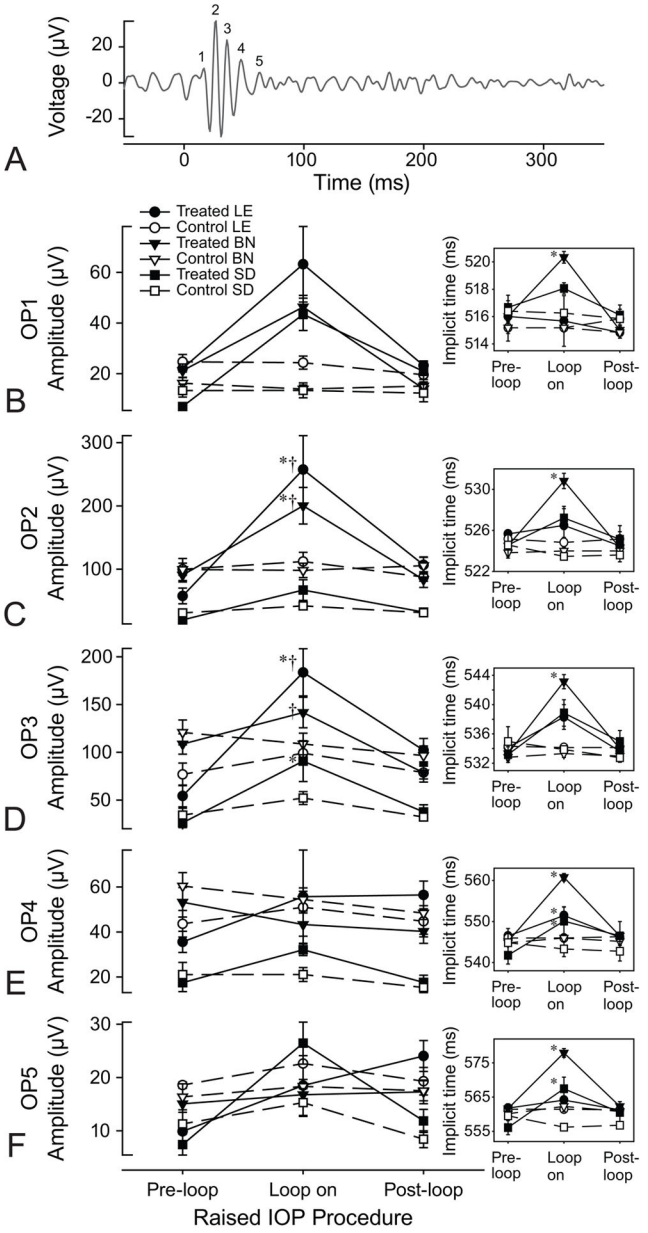

Fig. 4.

OP amplitudes and implicit times of the three rat strains. (a) Sample OP from a LE rat at a luminance of −3.04 log cd·s/m^2. Flash onset is at 0 ms. (b–f) Mean OP1−5 amplitudes for each rat strain, treated and control eyes, pre-during and post-IOP elevation. Error bars are standard error of means. The insets reflect mean OP implicit times for each strain, eye and loop condition. Asterisks (*) indicate differences relative to pre-loop conditions for the rat strain. Daggers (†) reflect a significant difference relative to SD rats at the same loop-condition.

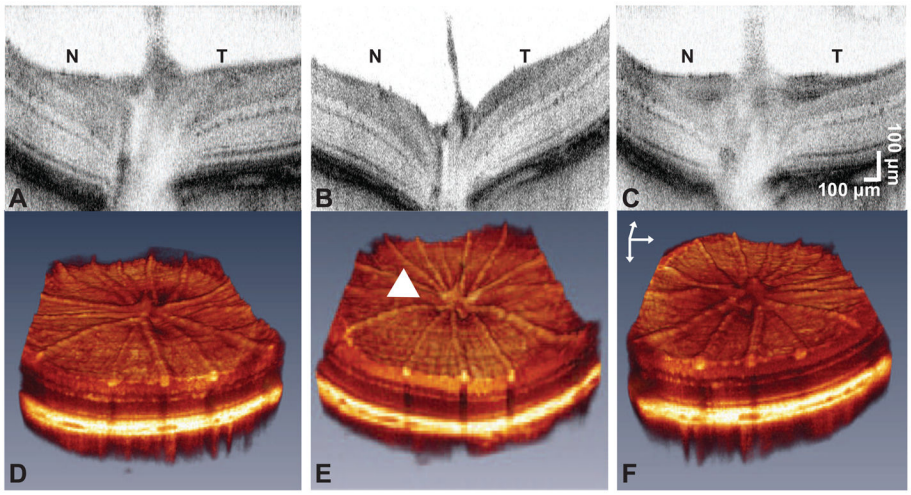

Fig. 5.

UHR-OCT images in response to IOP elevation. (a, b and c) Two-dimensional and (d, e and f) three-dimensional representative, UHR-OCT images of a LE treated rat retina, (a and d) before, (b and e) during and (c and f) after IOP elevation. The arrow head indicates the region of backward bowing during IOP elevation. Scale bars: z = 400 µm, x and y = 200 µm. 'N' is nasal and 'T' is temporal with respect to the orientation of the image.

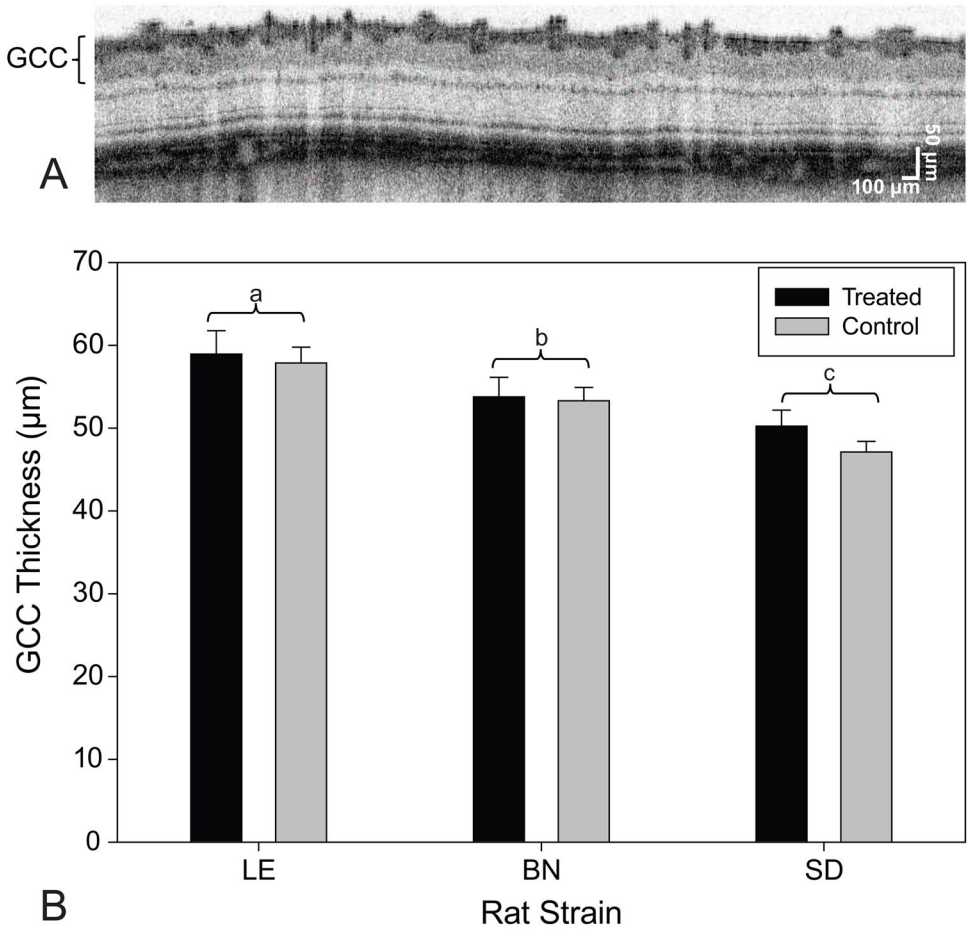

Fig. 6.

GCC thicknesses of the three rat strains. (a) Representative cross-sectional UHR-OCT image acquired from a circular scan centered at the ONH of a treated LE rat retina prior to IOP elevation. (b) Mean GCC thicknesses for each rat strain for both the treated and the control eyes. LE had the thickest GCCs followed by BN and SD rats. Error bars are standard deviation. Letters ‘a’, ‘b’, and ‘c’ represent significant differences between other strains.

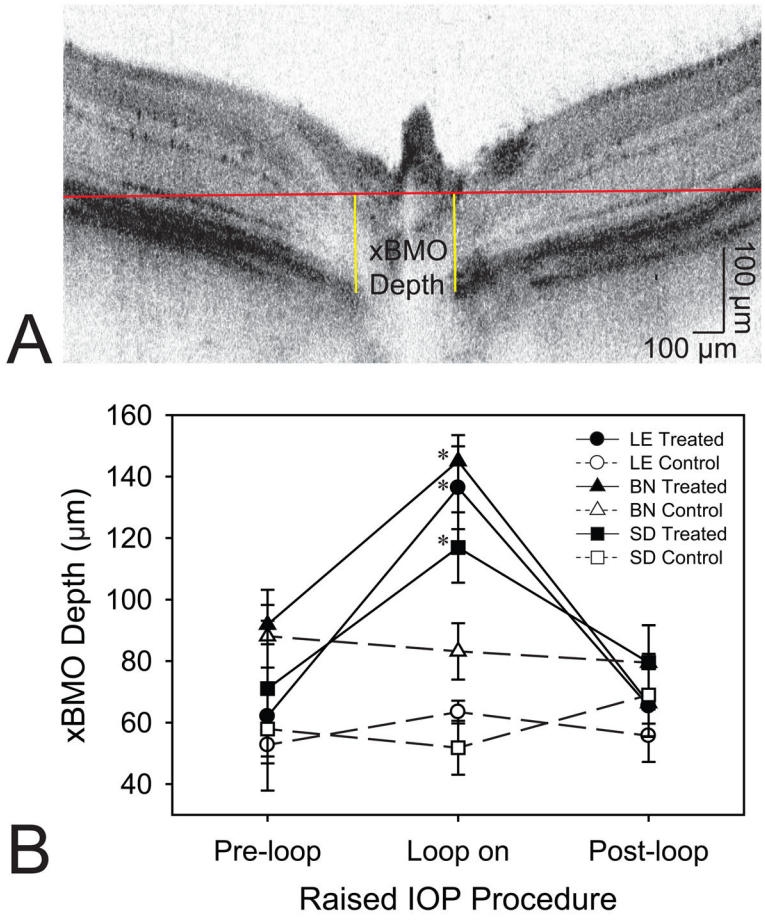

Fig. 7.

Structural changes in the rat retina in response to elevated IOP. (a) Graphical representation of the method used for determining the xBMO. The sample image is from a LE rat during IOP elevation. (b) Mean xBMO depth for each rat strain, treated and control eye, and pre-, during and post-IOP elevation. Error bars are standard error of means. Asterisks (*) indicate differences relative to pre-loop conditions for the rat strain.

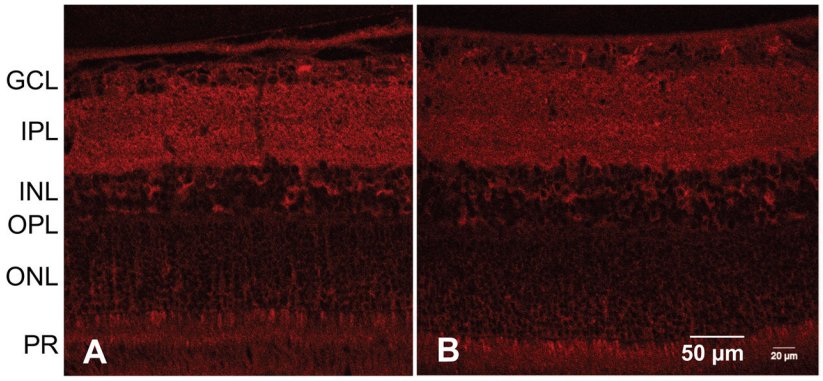

Fig. 8.

Immunohistochemical staining of representative rat retinas for LC3. LC3 was equally expressed throughout the retinal section of a (a) treated and (b) control eye from a BN rat. GCL = ganglion cell layer, IPL = inner plexiform layer, INL = inner nuclear layer, OPL = outer plexiform layer, ONL = outer nuclear layer, PR = photoreceptor layer.

Table 1

Mean IOP (± standard deviation) for each experimental procedure for each rat strain (LE = Long-Evans, BN = Brown Norway, SD = Sprague-Dawley). IOP values are those recorded before the loop was put on (pre-loop), 30 minutes after the loop was placed on (loop on) and 30 minutes after the loop was removed (post-loop).

Procedure	Eye	Strain	IOP (mean ± SD mmHg)		
			Pre-loop	Loop on	Post-loop
STR	Treated	LE	11.3 ± 0.5	35.4 ± 2.2	8.3 ± 0.5
		BN	10.8 ± 1.1	33.7 ± 2.1	7.2 ± 0.6
		SD	12.9 ± 1.1	29.6 ± 1.6	7.6 ± 0.4
	Control	LE	10.5 ± 0.9	9.2 ± 0.6	8.3 ± 7.9
		BN	10.8 ± 0.4	9.3 ± 0.4	7.9 ± 0.9
		SD	11.9 ± 1.1	10.1 ± 0.7	9.9 ± 0.4
ERG	Treated	LE	9.7 ± 0.6	37.6 ± 2.3	8.5 ± 0.6
		BN	8.2 ± 0.3	36.6 ± 1.1	6.7 ± 0.4
		SD	7.5 ± 0.6	33.7 ± 1.5	8.0 ± 1.2
		LE	9.3 ± 0.7	8.9 ± 0.2	10.3 ± 0.4
	Control	BN	9.0 ± 0.4	9.3 ± 0.6	8.6 ±0.4
		SD	9.1 ± 1.3	7.8 ± 0.5	7.5 ± 0.7
UHR-OCT	Treated	LE	9.1 ± 0.5	36.3 ± 1.7 †	8.9 ± 0.6
		BN	8.9 ± 0.4	31.3 ± 0.9	7.7 ± 0.6
		SD	9.1 ± 0.6	32.1 ± 2.9	6.3 ± 0.3
	Control	LE	9.7 ± 0.9	11.1 ± 0.5	12.0 ± 1.1
		BN	8.7 ± 0.2	9.2 ± 0.6	8.9 ± 0.3
		SD	9.4 ± 0.3	10.9 ± 0.6	8.9 ± 0.7

Strain-dependent differences in IOPs were observed only for the treated eyes during loop-wear. Daggers (†) reflect a significant difference relative to SD rats at the same loop-condition (P=0.0002). Please see text for more comparisons.

Table 2

Summary of strain-dependent differences in STR, ERG, and UHR-OCT data (LE = Long-Evans, BN = Brown Norway, SD = Sprague-Dawley). Letters 'a', 'b', and 'c' represent significant differences between other strains.

	Treated Eye			Control Eye		
Component	**Prior to IOP elevation**	**During IOP elevation**	**Post IOP**	**Prior to IOP elevation**	**During IOP elevation**	**Post IOP**
STR amplitudes	none	LE(a)=BN(a)>SD(b)	none		none	
STR implicit times	none	LE(a)<BN(b)=SD(b)	none		none	
ERG-a wave amplitudes	none	LE(a)=BN(a)>SD(b)	none		none	
ERG a-wave implicit times	none	LE(a)=BN(a)>SD(b)	none		none	
ERG b-wave amplitudes	none	LE(a)=BN(a)>SD(b)	none		none	
ERG b-wave implicit times	none	LE(a)=BN(a)<SD(b)	none		none	
OP1, OP4 amplitudes			none			
OP1, OP4 implicit times			none			
OP2 amplitudes			LE(a)=BN(a)>SD(b)			
OP2 implicit times			none			
OP3 amplitudes *	BN(a)>LE(b)=SD(b)	LE(a)=BN(a)>SD(b)		BN(a)>LE(b)=SD(b)	LE(a)=BN(a)>SD(b)	
OP3 implicit times			none			
OP5 amplitudes			none			
OP5 implicit times	none	BN(a)>LE(b)=SD(b)	none		none	
xBMO			none			
GCC Thickness	LE(a)>BN(b)>SD(c)	n/a		LE(a)>BN(b)>SD(c)	n/a	
Total Retinal Thickness	LE(a)>BN(b)=SD(b)	n/a		LE(a)>BN(b)=SD(b)	n/a	

* no differences were observed between eyes for all loop conditions

Table 3

Mean total retinal thickness (Mean ± standard deviation) for each rat strain (LE = Long-Evans, BN = Brown Norway, SD = Sprague-Dawley) with respect to treated and control eyes at baseline.

Eye	Total Retinal Thickness (mean ± standard deviation μm)		
	LE	BN	SD
Treated	160.9 ± 11.1	152.5 ± 9.8	154.8 ± 11.6
Control	165.3 ± 5.3	152.7 ± 4.1	154.1 ± 11.0

LE rats had the thickest retinas than compared to BN or SD rats (P=0.04543 for LE vs BN, P=0.0280 for LE vs SD, while BN and SD rat retinal thicknesses did not significantly differ (P=0.9599).